Published in final edited form as:
J Pharm Sci. 2011 August ; 100(8): 3345–3356. doi:10.1002/jps.22529.

Formulation of Tenofovir-Loaded Functionalized Solid Lipid Nanoparticles Intended for HIV Prevention

DIMA ALUKDA[1], **TIMOTHY STURGIS**[2], and **BI-BOTTI C. YOUAN**[1]

[1] Laboratory of Future Nanomedicine and Theoretical Chronopharmaceutics, Division of Pharmaceutical Sciences, University of Missouri-Kansas City, Kansas City, Missouri 64108

[2] Department of Environmental Health and Safety, University of Missouri-Kansas City, Kansas City, Missouri 64110

Abstract

The objective of this study is to engineer polylysine–heparin functionalized solid lipid nanoparticles (fSLNs) for the use of a vaginal microbicide delivery template for HIV prevention. The fSLNs are prepared using a modified phase-inversion technique followed by a layer-by-layer deposition method. The Box–Behnken experimental design is used to analyze the influence of three factors (X_1 = bovine serum albumin concentration, X_2 = pH of the aqueous phase, and X_3 = lipid amount) on the particle mean diameter (PMD) measured by dynamic light scattering (DLS). Tenofovir is used as a model anti-HIV microbicide. The SLNs are also characterized for morphology, zeta potential (ζ), percent drug encapsulation efficiency (EE%), and cytotoxicity on a human vaginal epithelial cell line by electron microscopy, DLS, ultraviolet, and fluorescence spectroscopy, respectively. The statistical model predicts particle size (Y) with 90% confidence and the Y values are significantly affected by X_1 and X_2. The produced fSLNs appear noncytotoxic and exhibit a platelet-like shape with respective PMD, EE%, and ζ value of 153 nm, 8.3%, and −51mV. These fSLNs intended to be administered topically have the potential to enhance cellular uptake of hydrophobic microbicides and outdistance the virus during the HIV/AIDS infection process, possibly leading to more effective prevention of the disease transmission.

Keywords

coating; colloids; formulation; functionalization; HIV prevention; lipids; nanoparticles; tenofovir; topical drug delivery

INTRODUCTION

The HIV epidemic is still a global health problem that continues to grow. According to the UNAIDS 2008 report, there were an estimated 33 million people living with HIV in 2007.[1] However, currently available microbicides, such as gels, lack the ability to provide an effective and long-lasting drug barrier along the epithelial mucosa suggesting the need for alternative vaginal formulations.[2–6] Therefore, there is a necessity for the use of innovative nanocarriers to overcome the previous limitations of conventional microbicide formulations.[4] Thus, the exploitation of nanocarriers of antiretroviral drugs is particularly advantageous for targeted delivery to cells or organs that are implicated in HIV transmission.[7] Previous studies have shown that the use of nanotechnology has increased the uptake of the chemokine N-alpha-(nonanoyl)-des-Ser-1 [L-thioproline-2, L-alpha-

Correspondence to: Bi-Botti C. Youan (Telephone: +816-235-2410; Fax: +816-235-5779; youanb@umkc.edu).

cyclohexyl-glycine-3]-RANTES (PSC-RANTES) into vaginal epithelial tissue.[8] Tenofovir (TNF), a nucleotide analog HIV-1 reverse transcriptase inhibitor is currently administered orally in its prodrug form, tenofovir disoproxil fumarate (TDF). TDF is effective against a range of HIV-1 subtypes, as well as CCR5-using and CXCR4-using HIV-1.[9] It also has a long intracellular half-life, low risk of resistance development,[10] and has been proposed for use in pre-clinical trials as a microbicide.[11]

A formulated topical gel (1% TNF) applied rectally has been shown to offer 67% protection after using a single, high-dose challenge model with rhesus macaques.[10,12] Moreover, some recent studies showed that using TNF in a microbicide formulation will not enhance the transmission of HIV, neither through disrupting the epithelium nor through other inflammatory responses.[13] Those promising results made TNF a good anti-HIV model to be encapsulated into functionalized solid lipid nanoparticles (fSLNs) for a potential vaginal microbicide delivery for the prevention of HIV transmission.

Solid lipid nanoparticles were selected over other nanoparticle constructs because they provide numerous potential advantages, including the possibility of controlled release of drug and drug targeting, an increase in drug stability, the ability of incorporating both lipophilic and hydrophilic drugs, and their biocompatibility.[14] The later advantage is due to the fact that SLNs are made of either physiological lipids or from lipids that are commonly used as pharmaceutical excipients.[15] There are increasing scientific evidence supporting that certain lipids are able to inhibit both presystemic drug metabolism and P-glyoprotein-mediated drug efflux.[16] Moreover, SLNs have been used in pharmaceutical formulation to enhance the penetration of bioactive agents into the epidermis.[17] These studies suggest that SLNs could enhance topical penetration of bioactive agents. In addition, SLNs could be easily functionalized by adding different ligands (cell penetration peptides, i.e., polylysine or PLL and bioactive polysaccharides, i.e., heparin) onto the surface; hence allowing SLNs to reach the subendothelium.[18]

The rationale for the selected ingredient (PLL and heparin) for the SLN functionalization was multifactorial. First, it has been shown that natural cytotoxic receptors (NCRs), such as NKp46 (Ref. 19), and killer lectin-like receptors (NKG2D and CD94)[20] are expressed by natural killer (NK) cells. These NCRs can bind to heparin- and sulfate-containing polysaccharides and potentially mediate the direct killing of virus-infected cells by NK cells for enhanced prevention of HIV transmission. Second, the PLL has a long-established reputation of enhancing intracellular uptake of several compounds.[21,22] Third, the interaction of heparin is documented, specifically with the cell-surface components of a human uterine epithelial carcinoma cell line.[23] Fourth, the PLL–heparin complex efficiency in macromolecular drug transport is demonstrated.[24] Fifth, based on lessons learned from viral infection process of cells, it was rationalized that the high density of surface charge creates a hydrophilic surface that minimizes hydrophobic entrapment to mucus.[25] Thus, based on the foregoing background informations, we hypothesize that the selected macromolecules for surface functionalization would enhance microbicide uptake for improved HIV prevention.

In this study, Box–Behnken experimental design (BBD) was used for screening formulation variables allowing minimizing the SLN size. Smaller sized and hydrophilic nanoparticles (<500 nm)[26] would facilitate diffusion and penetration into the mucus layer lining the vaginal epithelia, keeping in mind that these SLNs were intended to reach the subepithelial layer and penetrate the vaginal cell lines. To our knowledge, this is the first time that fSLNs have been engineered for a topical delivery of a vaginal microbicide. For this reason, it is important to set up a preliminary toxicity study to evaluate the effect of this nanoformulation

on the vaginal epithelial cell line, as safety is an important property of any microbicide formulation[3]

MATERIALS AND METHODS

Materials

The Softisan 100 was kindly provided as a gift from SASOL (Sasol North America Inc., Westwood, New Jersey, USA). The bovine serum albumin (BSA), poly(L-Lysine hydrochloride) (PLL) molecular weight (MW; 22,100 Da), and poly(acrylic acid) (PAA) MW ~10,000 Da) were purchased from Sigma–Aldrich, (St. Louis, Missouri, USA). The low-molecular-weight heparin (LMWH, lot PH 61807 @ 170 IU mg^{-1}) was obtained from Celsus (Cincinnati, Ohio, USA). The TNF was purchased from Zhongshuo Pharmaceutical Co. Ltd. (Beijing, China). The acetone and dimethyl-sulfoxide (DMSO) were from Fisher Scientific (Pittsburgh, Pennsylvania). Float-A-Lyzer dialysis membranes [cellulose ester, 100K, molecular weight cutoff (MWCO)] were from Spectrum Laboratories (Rancho Dominguez, California, USA).

The human vaginal epithelial cell line VK2/E6E7 was from American Type Culture Collection (ATCC, Boston, Massachusetts, USA). Keratinocytes–SFM serum-free medium was from GIBCO Invitrogen (Carlsbad, California, USA), the medium composition was modified to reach the desired calcium concentration by adding $CaCl_2$ (0.4 mM) 155 μL/100 mL medium, recombinant epidermal growth factor (0.1 ng/mL), (2.69 μL/100 mL), and bovine pituitary extract (400 μL/100 mL).

The CellTiter 96® AQueous nonradioactive cell proliferation assay [3-(4,5-dimethylthiazol -2-yl)-5-(3-carboxymethoxyphenyl)-2-(4-sulfophenyl)-2H-tetrazolium, inner salt; MTS] and lactate dehydrogenase (LDH) cell cytotoxicity kit (CytoTox-ONE™, Homogeneous Membrane Integrity Assay) were from Promega (Madison, Wisconsin, USA). All other chemicals used in this study were of analytical grade and used without further purification.

Synthesis of Functionalized SLN

The functionalized SLNs or fSLNs were prepared by a modified phase-inversion process as previously described by Jayagopal et al.[18] In this process, a known amount (Table 1) of Softisan and 1 mg of TNF were dissolved in 1 mL of organic phase that consisted of acetone: DMSO (60:40) volume mixture. This mixture had a solvent polarity–polarizability index (SPP) of 92.8 as calculated according to Catalan et al.[27] The organic mixture was then added to 1 mL of an aqueous phase that has one of the three levels of BSA concentration (Table 1) and 0.001% (w/v) of the first surface functionalizing moiety (PAA). The pH of the aqueous phase indicated in Table 1 was adjusted using 0.1 N HCl. The system was manually and gently shaken for 30 s. The excess BSA, residual solvents, and PAA were removed by dialysis against 1 L of deionized water for 4 h, with three water changes. Additional layers of macromolecules (PLL and finally heparin) were added according to the electrostatic layer-by-layer assembly method.[28] In this study, the SLNs were first synthesized without functionalization in the 15 runs of the BBD for size optimization as described below, where three formulation variables were chosen (concentration of BSA in the aqueous phase, pH of the aqueous phase, and the amount of Softisan in organic phase). The fSLN was prepared from the SLNs with minimal size and had three layers of macromolecules from inside out: PAA, PLL, and heparin, respectively.

Assessment of Size and Zeta Potential of SLNs

The average size, size distribution, and zeta potential (ζ) were determined using the dynamic light scattering (DLS) method with the Zetasizer Nano ZS series from Malvern Instruments

Ltd. (Worcestershire, United Kingdom). After suspending 100 μL of SLN suspension in 1 mL of deionized water and then sonicating for 30 s, the measurements were undertaken at a temperature of 25°C. The particle mean diameter (PMD) was represented as *Z*-average diameter following the cumulant model.[29–31] According to the National Institute Standard, a sample with a poly-dispersity index (PDI) of less than 0.05 is considered monodispersed.[32] The ζ value of the SLN suspension was measured using the ζ analysis mode of the instrument. Smoluchowski's approximation was used for the conversion of electrophoretic mobility into ζ according to the manufacturer's protocol. Nanosphere™ size standard (59 ± 2.5 nm) and ζ standard (−68 ± 6.8 mV) were used to calibrate the instrument prior to the analysis. The addition of the layers was proven by the change in ζ values after the addition of each layer. The ζ potential of the SLN was measured after the addition of each functionalizing moiety.

Transmission Electron Microscopy

Samples containing SLNs and fSLNs were diluted with 100 mM KCl to the concentration of 0.01 mg/mL, then the solution was sonicated for 30 s and mounted on a copper mesh, carbon-covered grid, and stained with 2% uranyl acetate. The excess fluids were dabbed off with filter paper. Finally, the samples were imaged with a JEOL 1200 EXII transmission electron microscope (JEOL of USA, Peabody, MA, USA), at magnifications of 10–50K, and recorded on film (Kodak SO163, Rochester, NY, USA).

Box–Behnken Experimental Design

The BBD was used to study the influence of the selected three factors or formulation variables on the particle size. BBD offers the advantage of exploring three experiment variables with three different levels without doing the experiment in extreme conditions.[32] In this study, the three formulation factors at their low, medium, and high levels and their responses are depicted in Table 1. Basically, 12 runs were performed along with three replicates at the center point. The polynomial equations and statistical analysis were performed via the eighth version of JMP statistical discovery software (Cary, North Carolina). The resulting statistical model was then checked with two random points of respective (X_1, X_2, X_3) values of (0.5, 0.5, 0.5), (−0.5, −0.5, 0) in addition to the theoretically optimal point. These checkpoints were performed in triplicates to ensure reproducibility. Using the Student's *t* test, the experimental responses (*Y*) were compared with those predicted by the model.

Encapsulation Efficiency

The EE% was measured at a wavelength of 260 nm by UV spectrometer (Spectronic Genesys 10 Bio, Thermo Electron Corporation, Wisconsin). The standard curve of the TNF was prepared using a drug concentration ranging from 2 to 100 μg/mL. The amount of encapsulated drug was calculated using mass balance by subtracting the amount of the free drug present in the supernatant from the total drug amount initially added in the preparation medium. The standard curve was $y = 0.0446x + 0.0052$ ($R^2 = 0.9993$) for TNF. The molar absorptivity of TNF was reported to be 1.586×10^4 L/mol/cm.[33]

Cytotoxicity Studies

The cell viability was determined by a DTX 800 multimode microplate reader (Beckman Coulter, Brea, California). Cells were seeded to 96-well plates, to ensure 1×10^4 cells per well, until 80% confluence was reached. The medium was changed with 100 μL medium of blank SLN. The concentration of SLNs in the cell culture medium ranged from 400 to 6000 μg/mL using three wells for each concentration. The plates were then incubated for 48 h. The medium was used as the negative control and 1% Triton X as the positive control.

Twenty microliters of the MTS solution was added to each well and incubated for 1 h at 37°C. The absorbance of the plates was monitored at the wavelength of 490 nm. After that, cell viability was determined using Eq. 1:

$$\text{Viability}\ (\%)=\frac{\text{ABS}_{\text{test}}}{\text{ABS}_{\text{control}}}\times 100 \quad (1)$$

where ABS_{test} and $\text{ABS}_{\text{control}}$ represented the amount of formazan detected in viable cells.

The cellular membrane integrity was determined by the release of LDH. Briefly, cells were seeded in 96-well plates and incubated with the SLNs and fSLNs using the same condition as stated above. One row of a 96-well plate without cells was used to determine if there was a background fluorescence and at what wavelength. At different time intervals, the plates were equilibrated to 22°C and 100 μL of CytoTox-ONE™ reagent was added to each well. The plates were incubated at 22°C for 10 min, and then 50 mL of stop solution was added to each well. The fluorescence was detected using the above microplate reader at an excitation wavelength of 560 nm and emission wavelength of 590 nm. The percent cytotoxicity for a given treatment was expressed using Eq. 2:

$$\text{Cytotoxicity}(\%)=100\times\frac{\text{experimental}-\text{background}}{\text{positive}-\text{background}} \quad (2)$$

where experimental, background, and positive represent the absorbance of SLN-treated wells, background control wells containing cells not treated with SLNs or fSLNs, and positive control wells containing cells treated with 1% Triton X, respectively.

RESULTS AND DISCUSSION

BBD Statistical Analysis and Optimization Before Functionalization

Table 2 shows SLN hydrodynamic diameter values obtained for the 15 runs with the corresponding PDI values. The SLNs were synthesized first without the functionalization steps following the method mentioned above. DMSO was chosen because it is the suitable solvent for TNF. The size expressed as *Z*-average mean diameter of the desired nanoparticles was chosen as the primary response because the goal of the study was to minimize the particle size. The *Z*-average diameter, sometimes called the cumulants mean or hydrodynamic diameter, is the mean diameter calculated from the Brownian motion of the particles. This diameter is intensity weighted and is therefore sensitive to the presence of large particles. It was chosen (as opposed to D_{10}, D_{90}) because it is a suitable parameter for following processes such as particle aggregation or crystallization. The produced SLNs had a size range between 220 and 734 nm. The PDI data also showed that the SLNs were also polydispersed, which is not uncommon for SLNs.[34] The large PDI may be attributed to the presence of multiple populations of particles with different shapes (platelets and spherical), some of which exhibit larger size (>200nm).[35] It is noteworthy that the estimations of the particle size and PDI were based on the intensity of the light signal processed according to the cumulant method.[30] The cumulants K_i are defined as the coefficients of an expansion of a MacLaurin series. The PDI is given by the following Eq. 3:

$$\text{PDI}=\frac{K_2}{K_1^2} \quad (3)$$

where the cumulant K_1 is an effective mean diffusion coefficient, whereas K_2 describes the relative width of the size distribution if normalized by K_1.[30] These PI results were consistent with the morphological analysis below.

The analysis of data of BBD 15 runs gave the following polynomial Eq. 4 for SLN size:

$$Y=404+13X_1-14.125X_2+64.125X_3-112.5X_1X_2-53.5X_1X_3-3.75X_2X_3+108.625X_1^2+39.875X_2^2-142.125X_3^2 \quad (4)$$

where X_1, X_2, and X_3 are the coded variables (BSA concentration, pH of the aqueous phase, and amount of Softisan 100 in the organic phase, respectively).

Tables 3 and 4 show the analysis of variance and the lack of fit analysis, respectively, from which it appears that the correlation coefficient (R^2) value of Eq. 1 was 0.89 with a p value of 0.06. According to the published acceptability criteria for nanoencapsulation process,[36] a p value of less than 0.1 and R^2 value of more than 0.7 but less than 0.9 is required. Because the results fit within this range, the lack of fit analysis will need to determine the acceptability of the model. For the model to be accepted, the p value in the lack of fit analysis should be more than 0.1. The p value in this model is 0.426 (more than 0.1), thus the model is suited to represent the experimental data for the SLN average diameter with a 90% confidence level. Therefore, Eq. 1 could reasonably predict the SLN size based on the variables selected for this study. It also gives an insight on the change of SLN's size when two of these three variables change simultaneously. In Eq. 1, a positive coefficient before the term indicates an increasing effect on the particle size (Y), whereas a negative coefficient indicates a decreasing effect on Y.

To understand the significance of the effect of the selected variables and their interaction on the SLN's size, a Pareto chart was constructed as shown in Figure 1. This figure shows the effects of the formulation variables and their interaction on SLN size. On the chart, the horizontal axis represents the so-called standardized effects, which are in fact the t values. Those values are obtained based on the estimate of factor effect E_x, which was the coefficient in Eq. 1. Then, t values were calculated based on the following Eq. 5:

$$t=\frac{|E_x|}{SE_e} \quad (5)$$

where SE_e is the standard error of an effect.37

These standard effects are then compared with a tabulated value known as $t_{critical}$ = 2.571 (represented on the chart with a vertical line). $t_{critical}$ was determined at significance level of α = 0.05 for the residual degrees of freedom (df), where df = 5 (df = number of runs − number of terms − 1). Any factor for which the effect surpasses $t_{critical}$ would have a statistically significant effect on the particle size. According to the chart presented in Figure 1, only the terms: X_1 X_2, X_3^2, and X_1^2 have a statistically significant effect on the size. Thus, an increase in both the concentration of BSA (X_1) and pH (X_2) in the aqueous phase has a decreasing effect on the SLN size. This could be physicochemically explained by two hypotheses related to the charge density and/or to the pH-induced BSA conformation change. On the basis of first hypothesis, it is important to underscore that with the presence of a NH_2 and a COOH groups in its molecular structure, BSA is an amphiphilic protein. It also exhibits a different net charge at different environmental pH. The isoelectric point (pI) of BSA is 4.7, indicating that BSA has a positive charge below pI 4.7 and negative charge above pI 4.7.[38] The ξ of BSA at pH 7.0 was −18 mV.[39] The study of BSA adsorption on nanosized magnetic particles[38] suggest that higher pH combined with higher BSA concentration would possibly affect the adsorption pattern and packing, leading to dramatic decrease in particle size.

Assuming a simple aqueous nanosystem containing BSA, with the pH-induced BSA conformation change hypothesis, one should note that a lower pH (<2) changes the shape,

charge, and hydration of BSA[40] and its net charge. Thus at higher pH (>2), there are less denaturation and conformation changes of the BSA adsorbed on SLN surface, leading to smaller particle size. Moreover, these conformational changes promote aggregation in dimers and consequently increase the viscosity increment (the change in viscosity of the solution as a result of adding the solute molecules) of the solution.[41]

Equation 6 below shows that in a simple aqueous nanosystem, the increment viscosity changes when the shape of the molecule changes, and thus it increases as BSA is denatured by the low acidic pH (pH <2) into an elongated random coil molecule,[42,43] which will increase the v_h value and the shape factor V of BSA. Besides the reduced efficiency of the required mechanical energy for particle size reduction in a high viscosity environment, this increase in viscosity of the outer phase has been proven to reduce the diffusion rate of the solute molecules during the formation of the nanoparticles, resulting in larger sized nanoparticles.[44]

$$\frac{\eta_{sp}}{C} = \frac{VNv_h}{M} \tag{6}$$

where η_{sp} is the viscosity increment, C is the concentration of the solution, V is the shape factor, v_h represents the volume of the solution occupied by the hydrodynamic solute particle, N is Avogadro's number, and M is solute molar mass.[42] But in reality, the nanosystem under consideration is a more complex system. The influence of the solvent mixture (DMSO and acetone), drug eventually binding to polymer in the system, and PAA on the above responses remained to be elucidated.

From Figures 1 and 2, X_1^2 (BSA concentration) hada curvilinear effect on the particle size. Below the coded value of 0.318, there is a decrease in particle size with increasing BSA concentration perhaps due to the stabilizing effect of the BSA displaying a surfactant effect at low concentration. But above 0.318, particle size begins to increase due to the increased viscosity effect at a higher concentration.[45]

It also appears that the Softisan 100 concentration in the organic phase (X_3^2) had a curvilinear effect on particle size. At coded values below 0.199, the lipid amount appears to increase particle size, which is consistent with previous work performed with such lipids.[44] However, the reasons why the particle size begins to decrease after the coded value of 0.199 is attained remained to be elucidated and suggest a unique interaction between this lipid and the drug or BSA at higher concentration.

Checkpoint Analysis

The resultant model was then checked with two random points and the theoretically optimum point resulting from the statistical model with the three factors set at 0.318, 0.636, and 0.199. These runs were performed in triplicates; the results are shown in Table 5. The results show that the SLN sizes of the tested points were close to the predicted values. The differences between the predicted size values and the measured size values were statistically insignificant ($p > 0.05$) using the Student's t test. Indeed, for checkpoint 1, the result was $t = -0.57$, with a degree of freedom of df = 2 and $p = 0.63$; checkpoint 2 was $t = -1.42$, with df = 2 and $p = 0.29$; the optimum found in Figure 2 was $t = -2.33$, with df = 2 and $p = 0.14$. It was noteworthy that under these checkpoint conditions, the model was very flat because the optimally predicted size (407 nm) appeared to be close to the intercept (404 nm) of the model Eq. 3. Moreover, based on the Pareto Chart (Fig. 1), it was discussed above that only three terms out of 10 of the equations (namely X_1X_2, X_3^2, and X_1^2) had statistically significant influence. The other two checkpoints being close to the optimal point and

considering the pure experimental errors (31% of sum of square in Table 4) led to almost similar responses to that of the optimal value. Collectively, these *t* tests results show that the model prediction equation is an acceptable tool to predict the size of SLNs in this design space.

Functionalization and EE%

After setting the formulation parameters, the next step was to functionalize the optimally sized SLNs and measure their encapsulation efficiency. The experiment was performed in triplicates. The results of the three replicates of the optimum (O_1, O_2, and O_3) are shown in Table 6. The results showed that the functionalizing moieties were indeed being added as evidenced by the change in ζ after each macromolecule layer addition. The first layer consisted of PAA (a negative moiety), followed by the second layer (the positively charged PLL), and finally by the third layer (heparin, which is negatively charged). It was noteworthy that the size of the SLN was statistically significantly reduced only after adding the third layer of heparin ($p = 0.000329$). This observation can be explained by the heparin-induced condensation of the macromolecules on the particle surface. Moreover, further dialysis and dilution would make the residual solvent, incorporated in the supersaturated regions of the particles, diffuse into the aqueous phase,[44] and thus causing the size to shrink. This phenomenon could be similar to what was observed by Sjostrom et al.[46] for particles prepared by precipitation from oil-in-water emulsions. The encapsulation efficiency for the fSLNs was 8.3 ± 0.7% ($n = 3$). The predicted water solubility of TNF is 1.87 mg/mL, and its log *P* is −1.6.[47] Therefore, the low EE% could be attributed to relatively high TNF solubility in water, leading to dramatic drug loss in the water phase before the nanoparticles solidification and solvent removal. The reduction in particle size that increases the specific surface area could also be a contributing factor to the low EE%. Some of the approaches used to improve the encapsulation of such highly water-soluble compounds include the conjugation of the drug with the lipid itself to create as water-insoluble compound,[48] and ionic complexation with some molecules that are less water soluble such as dextran sulfate.[49] These alternative methods remained to be investigated in the search of effective means to improve the EE%.

Morphological Analysis

The transmission electron microscopy (TEM) for the unfunctionalized (Fig. 3a) and functionalized SLNs (Fig. 3b) showed a side view of platelet-shaped nanoparticles along with some apparently spherical particles. The apparently spherical SLNs could be either a top view of the platelet-shaped nanoparticles or actual spherical nanoparticles. However, the images qualitatively showed SLNs that are not uniformly sized. This observation correlates with the wide PDI values provided by DLS measurements. The platelet shape of the SLNs could be elucidated by the fact that Softisan 100 is composed of saturated fatty acid (C_{12}–C_{18}) triglycerides according to the manufacturer's product information sheet. Triglycerides exist in three different polymorphs (α, β prime, and β) that exhibit different shapes.[50] Although no heat was involved in the preparation procedure, the addition of DMSO to water is an exothermic reaction.[51] Thus, this addition caused an increase in temperature from room temperature to 33 ± 0.5° C. This increase in temperature might have caused (during the lipid crystallization and solidification phase) the polymorphic transition from α to β prime then to β forms. The latter is established to have a platelet-like shape.[52]

Cytotoxicity Study: Effect of Unfunctionalized and Functionalized SLN on the Vaginal Epithelial Cells Viability

It is required for topical formulation intended for the prevention of HIV infection to be safe for the patient.[53] Therefore, both MTS and LDH assays were employed to test the effect of SLNs on a vaginal epithelial cell line. As the safety of tenofovir gel (1%) has been

established in the literature,[9,54] these nanformulation templates were used without the drug to test the effects of the excipients used on the viability and cell membrane integrity of the selected vaginal epithelial cell line VK2/E6E7.

MTS is a tetrazolium compound that is bioreduced by viable cells into formazan. The amount of formazan produced is determined by measuring the absorbance at 490 nm, which is proportional with the number of living cells. Apparently, both unfunctionalized (Fig. 4) and functionalized formulations (Fig. 5) did not show any significant effect on cell viability compared with the cell culture medium (negative control). All the tested concentrations showed more than 80% cell viability compared with the positive control.

The LDH membrane integrity assay is a fluorimetric assay that is used to measure the release of LDH from cells with a disrupted membrane. Apparently, no significant LDH release has been observed in both unfunctionalized (Fig. 6) and functionalized SLN formulations (Fig. 7) with all the tested concentrations; LDH release was less than 15% from that of the positive control. There are some negative values presented in the assay that could be artifacts and are common in some LDH results presentations.[55,56]

Overall, in both the MTS and LDH assays, no significant difference was observed by the Student's *t* test, comparing data between the cell culture medium and those of the SLNs of different formulations and concentrations. These data indicate that the SLNs were not detrimental to vaginal epithelial cells. Because this specific nanosystem is intended for topical delivery, some comments relating the concentrations employed in this experiment to the potential required topical dose with respect to TNF content of the nanoparticles, and current topical doses are warranted. It has been reported that the *in vitro* EC_{50} of TNF was 5.0 ± 2.6 μM.[57] Considering that a vaginal suppository weighs approximately 5 g, and conservatively assuming a 20% (w/w) of fSLN in such a suppository, the ultimate vaginal formulation should be loaded with at least 17 μmol of TNF, leading to a vaginal drug concentration of 5.7 μM, given the fact that the average total volume of vaginal fluid and cervical mucus is 3 mL.[58] In the optimal conditions, even with this relatively low EE of approximately 8.3%, the drug loading is approximately 83 μg per 100 mg of fSLN. For a 20% (w/w) suppository content in fSLN, the drug content would be approximately 830 μg in 3 mL vaginal fluid potentially leading to a local concentration significantly above the median effective concentration (EC_{50} ~963 μM assuming a 100% burst release rate) while maintaining safety (100 mg/3 mL is still lower than the safe range tested). Remember that the current TNF tablet intended for oral administration contains 245–300 mg of drug. Thus, significant saving in final microbicide product cost is anticipated perhaps potentially leading to affordable drug cost for developing countries (with HIV prevalence) with such a localized and controlled nanomedicine-based delivery system if effective and safe supplies and processes are genuinely identified and used. Therefore, it can be reasonably speculated that such microbicide-loaded fSLN would potentially be affordable and exhibit an anti-HIV effect. However, this remains to be elucidated in the future in the *in vitro* and *in vivo* efficacy assay.

CONCLUSION

In this study, for the first time, tenofovir (TNF, an anti-HIV microbicide) was loaded in solid lipid nanoparticles (SLNs) intended for vaginal or topical drug delivery for the prevention of HIV/AIDS transmission. A modified phase-inversion technique was adopted to prepare the SLNs using response surface methodology. A statistical model that predicted the SLN size was acceptable with a 90% confidence level. The size-minimization goal (<500 nm) was successfully achieved with the production of fSLN of average diameter of 153 nm. The SLNs were functionalized successfully using a layer-by-layer technique. The

electron microscopies showed platelet-shaped SLNs in the size range that was consistent with the DLS measurements. The cytotoxicity assays showed a non-cytotoxic effect on vaginal epithelial cells for 48 h. Although the EE% was relatively low, the SLNs appear to be a promising drug delivery template for microbicides that are more hydrophobic. The SLNs can be effectively functionalized to potentially reach the subepithelial layer, offering the microbicide to a wider range of cells. Ultimately, SLNs are worth for further studies in the quest of an alternative drug delivery system for intravaginal/topical delivery of HIV microbicides to hinder HIV transmission.

Acknowledgments

The work presented was supported by Award Number R21A1083092 from the National Institute of Allergy and Infectious Diseases. The content is solely the responsibility of the authors and does not necessarily represent the official view of the National Institute of Allergy and Infectious Diseases or the National Institutes of Health. We are also grateful to Dr. Edward Gogol (School of Biological Sciences, University of Missouri, Kansas City, Missouri) for his valuable collaboration and help in TEM imaging.

References

1. UNAIDS. [Access date: December 14th, 2010] 2008 Report on the global AIDS epidemic. 2008. Available at: http://wwwunaidsorg
2. Klasse PJ, Shattock R, Moore JP. Antiretroviral drug-based microbicides to prevent HIV-1 sexual transmission. Annu Rev Med. 2008; 59:455–471. [PubMed: 17892435]
3. Balzarini J, van Damme L. Microbicide drug candidates to prevent HIV infection. Lancet. 2007; 369(9563):787–797. [PubMed: 17336656]
4. du Toit LC, Pillay V, Choonara YE. Nano-microbicides: Challenges in drug delivery, patient ethics and intellectual property in the war against HIV/AIDS. Adv Drug Deliv Rev. 2010; 62(4–5):532–546. [PubMed: 19922751]
5. Rohan LC, Sassi AB. Vaginal drug delivery systems for HIV prevention. AAPS J. 2009; 11(1):78–87. [PubMed: 19194802]
6. Garg AB, Nuttall J, Romano J. The future of HIV microbicides: Challenges and opportunities. Antivir Chem Chemother. 2009; 19(4):143–150. [PubMed: 19374141]
7. Vyas TK, Shah L, Amiji MM. Nanoparticulate drug carriers for delivery of HIV/AIDS therapy to viral reservoir sites. Expert Opin Drug Deliv. 2006; 3(5):613–628. [PubMed: 16948557]
8. Ham AS, Cost MR, Sassi AB, Dezzutti CS, Rohan LC. Targeted delivery of PSC-RANTES for HIV-1 prevention using biodegradable nanoparticles. Pharm Res. 2009; 26(3):502–511. [PubMed: 19002569]
9. Rohan LC, Moncla BJ, Kunjara Na Ayudhya RP, Cost M, Huang Y, Gai F, Billitto N, Lynam JD, Pryke K, Graebing P, Hopkins N, Rooney JF, Friend D, Dezzutti CS. In vitro and ex vivo testing of tenofovir shows it is effective as an HIV-1 microbicide. PLoS One. 2010; 5(2):e9310.10.1371/journal.pone.0009310 [PubMed: 20174579]
10. Parikh UM, Dobard C, Sharma S, Cong ME, Jia H, Martin A, Pau CP, Hanson DL, Guenthner P, Smith J, Kersh E, Garcia-Lerma JG, Novembre FJ, Otten R, Folks T, Heneine W. Complete protection from repeated vaginal simian-human immunodeficiency virus exposures in macaques by a topical gel containing tenofovir alone or with emtricitabine. J Virol. 2009; 83(20):10358–10365. [PubMed: 19656878]
11. Palmer S, Margot N, Gilbert H, Shaw N, Buckheit R Jr, Miller M. Tenofovir, adefovir, and zidovudine susceptibilities of primary human immunodeficiency virus type 1 isolates with non-B subtypes or nucleoside resistance. AIDS Res Hum Retroviruses. 2001; 17(12):1167–1173. [PubMed: 11522186]
12. Cranage M, Sharpe S, Herrera C, Cope A, Dennis M, Berry N, Ham C, Heeney J, Rezk N, Kashuba A, Anton P, McGowan I, Shattock R. Prevention of SIV rectal transmission and priming of T cell responses in macaques after local pre-exposure application of tenofovir gel. PLoS Med. 2008; 5(8):e157. discussion e157. [PubMed: 18684007]

13. Mesquita PM, Cheshenko N, Wilson SS, Mhatre M, Guzman E, Fakioglu E, Keller MJ, Herold BC. Disruption of tight junctions by cellulose sulfate facilitates HIV infection: Model of microbicide safety. J Infect Dis. 2009; 200(4):599–608. [PubMed: 19586414]

14. Mehnert W, Mader K. Solid lipid nanoparticles: Production, characterization and applications. Adv Drug Deliv Rev. 2001; 47(2–3):165–196. [PubMed: 11311991]

15. Almeida AJ, Souto E. Solid lipid nanoparticles as a drug delivery system for peptides and proteins. Adv Drug Deliv Rev. 2007; 59(6):478–490. [PubMed: 17543416]

16. Wasan KM. The biological functions of lipid excipients and the implications for pharmaceutical products development. J Pharm Sci. 2009; 98(2):379–382. [PubMed: 18484625]

17. Chen H, Chang X, Du D, Liu W, Liu J, Weng T, Yang Y, Xu H, Yang X. Podophyllotoxin-loaded solid lipid nanopar-ticles for epidermal targeting. J Control Release. 2006; 110(2):296–306. [PubMed: 16325954]

18. Jayagopal A, Sussman EM, Shastri VP. Functionalized solid lipid nanoparticles for transendothelial delivery. IEEE Trans Nanobioscience. 2008; 7(1):28–34. [PubMed: 18334453]

19. Zilka A, Landau G, Hershkovitz O, Bloushtain N, Bar-Ilan A, Benchetrit F, Fima E, van Kuppevelt TH, Gallagher JT, Elgavish S, Porgador A. Characterization of the heparin/heparan sulfate binding site of the natural cytotoxicity receptor NKp46. Biochemistry. 2005; 44(44):14477–14485. [PubMed: 16262248]

20. Higai K, Imaizumi Y, Suzuki C, Azuma Y, Matsumoto K. NKG2D and CD94 bind to heparin and sulfate-containing polysaccharides. Biochem Biophys Res Commun. 2009; 386(4):709–714. [PubMed: 19555665]

21. Ryser HJ, Drummond I, Shen WC. The cellular uptake of horseradish peroxidase and its poly(lysine) conjugate by cultured fibroblasts is qualitatively similar despite a 900-fold difference in rate. J Cell Physiol. 1982; 113(1):167–178. [PubMed: 6127344]

22. Ryser HJ, Shen WC. Conjugation of methotrexate to poly(L-lysine) increases drug transport and overcomes drug resistance in cultured cells. Proc Natl Acad Sci U S A. 1978; 75(8):3867–3870. [PubMed: 279001]

23. Raboudi N, Julian J, Rohde LH, Carson DD. Identification of cell-surface heparin/heparan sulfate-binding proteins of a human uterine epithelial cell line (RL95). J Biol Chem. 1992; 267(17): 11930–11939. [PubMed: 1601862]

24. Shen WC, Ryser HJ. Poly(L-lysine) has different membrane transport and drug-carrier properties when complexed with heparin. Proc Natl Acad Sci U S A. 1981; 78(12):7589–7593. [PubMed: 6950400]

25. Lai SK, Wang YY, Hanes J. Mucus-penetrating nanoparticles for drug and gene delivery to mucosal tissues. Adv Drug Deliv Rev. 2009; 61(2):158–171. [PubMed: 19133304]

26. Lai SK, O'Hanlon DE, Harrold S, Man ST, Wang YY, Cone R, Hanes J. Rapid transport of large polymeric nanoparticles in fresh undiluted human mucus. Proc Natl Acad Sci U S A. 2007; 104(5):1482–1487. [PubMed: 17244708]

27. Catalan JL, Lopez V, Perez P. Solvent dipolarity polarizability (SPP) of alcoholic solvents. Liebigs Ann. 1995; 1995(5):793–795.

28. Decher G. Fuzzy nanoassemblies: Towars layered ploymeric multicomposites. Science. 1997; 277:1232–1237.

29. Koppel DE. Analysis of macromolecular polydispersity in intensity correlation spectroscopy: The method of cumulants. J Chem Phys. 1972; 57:4814–4820.

30. Katzel U, Vorbau M, Stintz M, Gottschalk-Gaudig T, Barthel H. Dynamic light scattering for the characterization of polydisperse fractal systems: II. Relation between structure and DLS results. Part Part Syst Charact. 2008; 25:19–30.

31. Kolchens S, Ramaswami V, Birgenheier J, Nett L, O'Brien DF. Quasi-elastic light scattering determination of the size distribution of extruded vesicles. Chem Phys Lipids. 1993; 65(1):1–10. [PubMed: 8348672]

32. Montgomery, DC. Response surface methods and design in design and analysis of experiments. New York: John Wiley and sons, Inc; 1995. p. 405-458.

33. Patel SB, US, Rajesh P, Prabhakar D, Engla G, Nagar PN. Spectrophotometric method development and validation for simultaneous estimation of tenofovir disoproxil fumarate and emtricitabine in bulk drug and tablet dosage form. Int J Pharm Clin Res. 1:28–30.
34. Muller RH, Mader K, Gohla S. Solid lipid nanoparticles (SLN) for controlled drug delivery—A review of the state of the art. Eur J Pharm Biopharm. 2000; 50(1):161–177. [PubMed: 10840199]
35. Blasi P, Giovagnoli S, Schoubben A, Ricci M, Rossi C. Solid lipid nanoparticles for targeted brain drug delivery. Adv Drug Deliv Rev. 2007; 59(6):454–477. [PubMed: 17570559]
36. Magenheim, B.; Benita, S. Microencapsulation, methods and industrial applications. New York: Marcel Dekker; 1996. The use of factorial design in the development of nanoparticulate dosage forms; p. 93-132.
37. Zhang T, Murowchick J, Youan BB. Optimization of formulation variables affecting spray-dried oily core nanocapsules by response surface methodology. J Pharm Sci. 2010:100.
38. Peng ZG, Hidajat K, Uddin MS. Adsorption of bovine serum albumin on nanosized magnetic particles. J Colloid Interface Sci. 2004; 271(2):277–283. [PubMed: 14972603]
39. Peters T Jr. Serum albumin. Adv Protein Chem. 1985; 37:161–245. [PubMed: 3904348]
40. Estey T, Kang J, Schwendeman SP, Carpenter JF. BSA degradation under acidic conditions: A model for protein instability during release from PLGA delivery systems. J Pharm Sci. 2006; 95(7):1626–1639. [PubMed: 16729268]
41. Curvale R, Masuelli M, Padilla AP. Intrinsic viscosity of bovine serum albumin conformers. Int J Biol Macromol. 2008; 42(2):133–137. [PubMed: 18022223]
42. Richards LJ. Viscosity and the shapes of macromolecules: A physical chemistry experiment using molecular-level models in the interpretation of macroscopic data obtained from simple measurements. J Chem Educ. 1993; 70(8):685–689.
43. Harrington WF, Johnson P, Ottewill RH. Bovine serum albumin and its behaviour in acid solution. Biochem J. 1956; 62(4):569–582. [PubMed: 13315216]
44. Schubert MA, Muller-Goymann CC. Solvent injection as a new approach for manufacturing lipid nanoparticles—Evaluation of the method and process parameters. Eur J Pharm Biopharm. 2003; 55(1):125–131. [PubMed: 12551713]
45. Wetzel R, Becker M, Behlke J, Billwitz H, Bohm S, Ebert B, Hamann H, Krumbiegel J, Lassmann G. Temperature behaviour of human serum albumin. Eur J Biochem. 1980; 104(2):469–478. [PubMed: 6244951]
46. Sjostrom B, Kaplun A, Talmon Y, Cabane B. Structures of nanoparticles prepared from oil-in-water emulsions. Pharm Res. 1995; 12(1):39–48. [PubMed: 7724486]
47. van Gelder J, Witvrouw M, Pannecouque C, Henson G, Bridger G, Naesens L, De Clercq E, Annaert P, Shafiee M, van Den Mooter G, Kinget R, Augustijns P. Evaluation of the potential of ion pair formation to improve the oral absorption of two potent antiviral compounds, AMD3100 and PMPA. Int J Pharm. 1999; 186(2):127–136. [PubMed: 10486430]
48. Olbrich C, Gessner A, Kayser O, Muller RH. Lipid-drug-conjugate (LDC) nanoparticles as novel carrier system for the hydrophilic antitrypanosomal drug diminazenediaceturate. J Drug Target. 2002; 10(5):387–396. [PubMed: 12442809]
49. Wong HL, Bendayan R, Rauth AM, Wu XY. Development of solid lipid nanoparticles containing ionically complexed chemotherapeutic drugs and chemosensitizers. J Pharm Sci. 2004; 93(8): 1993–2008. [PubMed: 15236449]
50. Sato K. Crystallization behaviour of fats and lipids—A review. Chem Eng Sci. 2001; 56:2255–2265.
51. Suzanne, M.; Watt, EA.; Armitage, Sue. Cryopreservation of hematopoietic stem/progenitor cells for therapeutic use. In: Day, JG.; Stacey, GN., editors. Cryopreservation and freeze-drying protocols. 2. Totowa, New Jersey: Humana Press Inc; 2007. p. 237-259.
52. Bunjes H, Steiniger F, Richter W. Visualizing the structure of triglyceride nanoparticles in different crystal modifications. Langmuir. 2007; 23:4005–4011. [PubMed: 17316032]
53. Lederman MM, Offord RE, Hartley O. Microbicides and other topical strategies to prevent vaginal transmission of HIV. Nat Rev Immunol. 2006; 6(5):371–382. [PubMed: 16639430]
54. Abdool Karim Q, Abdool Karim SS, Frohlich JA, Grobler AC, Baxter C, Mansoor LE, Kharsany AB, Sibeko S, Mlisana KP, Omar Z, Gengiah TN, Maarschalk S, Arulappan N, Mlotshwa M,

Morris L, Taylor D. Effectiveness and safety of tenofovir gel, an antiretroviral microbicide, for the prevention of HIV infection in women. Science. 2010; 329(5996):1168–1174. [PubMed: 20643915]

55. Williams, CM.; Bateman, PA.; Jackson, KG.; Yaqoob, P. 44th international conference on the bioscience of lipids; Oxford, UK: Keble College; 2003.
56. Takatori M, Kuroda Y, Hirose M. Local anesthetics suppress nerve growth factor-mediated neurite outgrowth by inhibition of tyrosine kinase activity of TrkA. Anesth Analg. 2006; 102(2):462–467. [PubMed: 16428543]
57. Lee WA, He GX, Eisenberg E, Cihlar T, Swaminathan S, Mulato A, Cundy KC. Selective intracellular activation of a novel prodrug of the human immunodeficiency virus reverse transcriptase inhibitor tenofovir leads to preferential distribution and accumulation in lymphatic tissue. Antimicrob Agents Chemother. 2005; 49(5):1898–1906. [PubMed: 15855512]
58. Sassi AB, Isaacs CE, Moncla BJ, Gupta P, Hillier SL, Rohan LC. Effects of physiological fluids on physical-chemical characteristics and activity of topical vaginal microbicide products. J Pharm Sci. 2008; 97(8):3123–3139. [PubMed: 17922539]

Sorted Parameter Estimates

Term	Estimate	Std Error	t Ratio	Prob>|t|
X1*X2	−112.5	35.94318	−3.13	0.0260*
X3*X3	−112.125	37.41085	−3.00	0.0302*
X1*X1	108.625	37.41085	2.90	0.0337*
X3	64.125	25.41567	2.52	0.0530
X1*X3	−53.5	35.94318	−1.49	0.1968
X2*X2	39.875	37.41085	1.07	0.3352
X2	−14.125	25.41567	−0.56	0.6023
X1	13	25.41567	0.51	0.6308
X2*X3	−3.75	35.94318	−0.10	0.9210

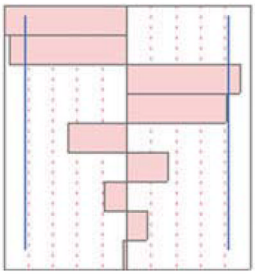

Figure 1.

Pareto chart depicting the standardized effect of formulation variables and their interactions on SLN size; horizontal axis shows the *t* ratio of the variables. Bars surpassing the two vertical lines indicate values reaching statistical significance ($\alpha = 0.05$). X_1, BSA concentration in the aqueous phase; X_2, pH of the aqueous phase; and X_3, Softisan 100 concentration in the organic phase.

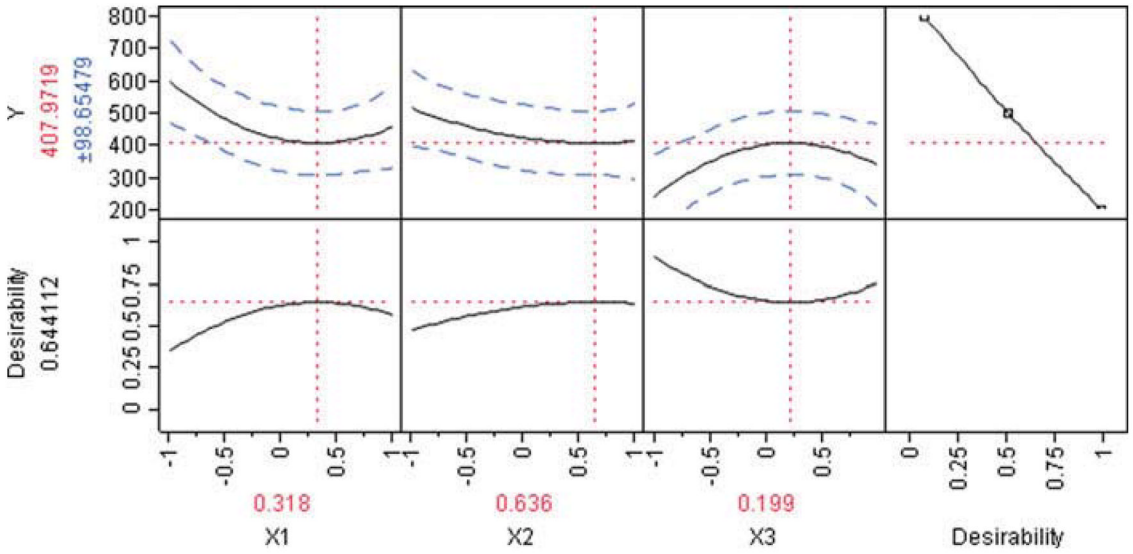

Figure 2.
Prediction profiler and desirability plot showing the effect of formulation variables on particle size (*Y*).

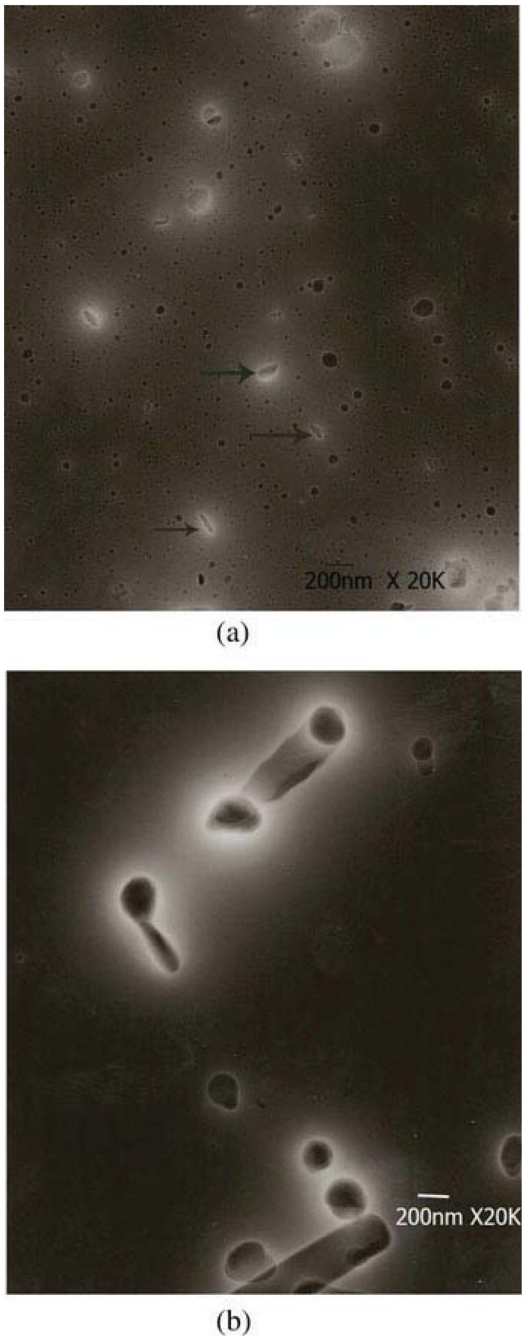

Figure 3.
Transmission electron microscopy image showing platelet-like shape for (a) unfunctionalized SLN with different sizes that reflect the polydispersity of SLN and (b) functionalized SLN (fSLN). Scale bars represent 200 nm.

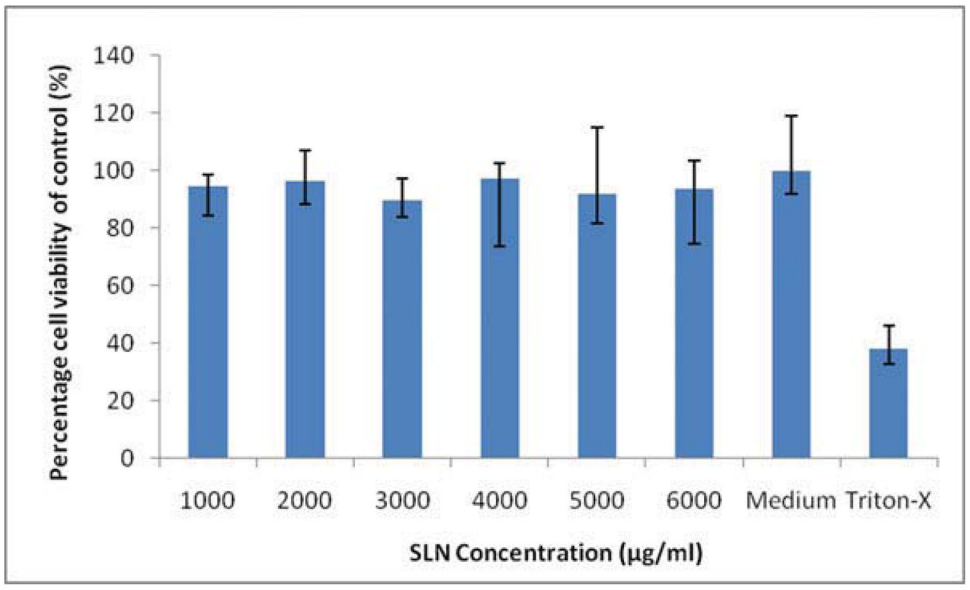

Figure 4.
Effect of various concentrations of unfunctionalized SLN on vaginal epithelial cells viability over 48 h period ($n = 3$).

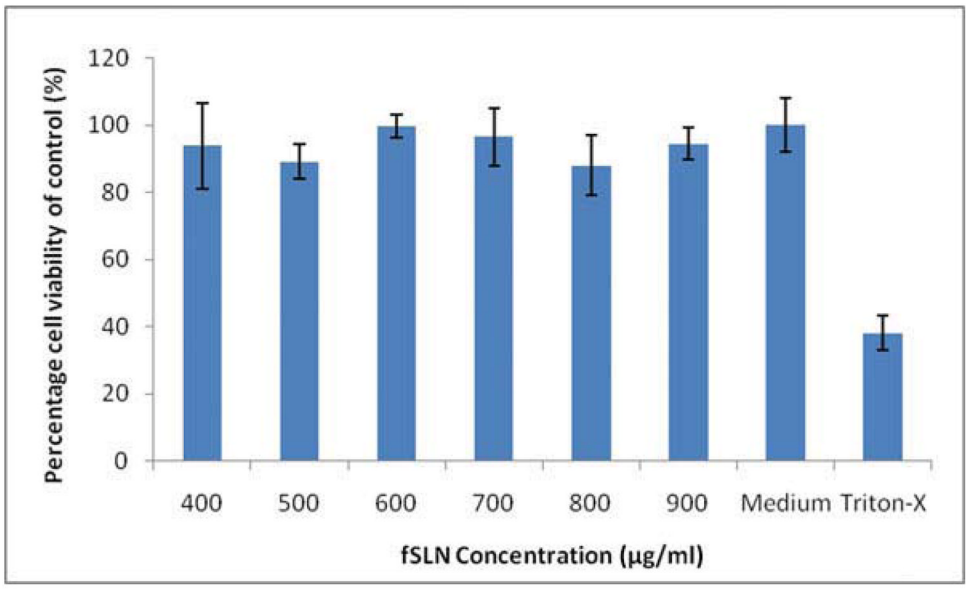

Figure 5.
Effect of various concentrations of functionalized SLNs (fSLNs) on vaginal epithelial cells viability over 48 h period ($n = 3$).

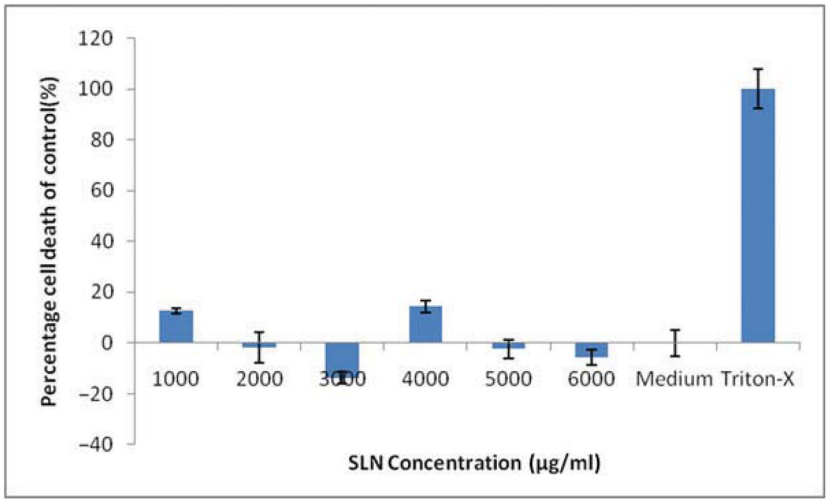

Figure 6.
Effect of various concentrations of unfunctionalized SLN on lactate dehydrogenase (LDH) release from vaginal epithelial cells over 48 h period ($n = 3$).

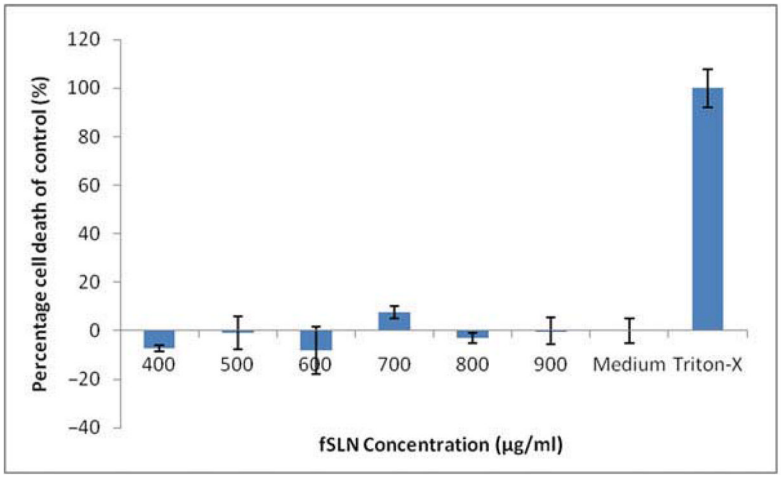

Figure 7.
Effect of various concentrations of functionalized SLNs (fSLNs) on lactate dehydrogenase (LDH) release from vaginal epithelial cells over 48 hours period ($n = 3$).

Table 1

Formulation Variables and Their Levels in the Experimental Design

Variables	Low	Medium	High
Independent variables			
X_1, BSA concentration (mg/mL)	1	5	9
X_2, pH of the aqueous phase	1	3	5
X_3, Softisan 100 amount (mg/mL)	1	10.5	20
Coded values	−1	0	+1

Dependent variable: Y_1, SLN's size (nm)

Table 2

Box–Behnken Experimental Design of Independent Variables with Measured Response

X_1	X_2	X_3	Particle Mean Diameter (nm)	Polydispersity Index
−1	−1	0	490	0.403
+1	−1	0	734	0.569
−1	+1	0	596	0.210
+1	+1	0	390	0.280
−1	0	−1	279	0.176
+1	0	−1	419	0.208
−1	0	+1	489	0.405
+1	0	+1	415	0.437
0	−1	−1	220	0.134
0	+1	−1	290	0.217
0	−1	+1	381	0.347
0	+1	+1	436	0.342
0	0	0	393	0.277
0	0	0	472	0.469
0	0	0	347	0.308

Table 3

Results of ANOVA of the Statistical Model Predicting Particle Mean Diameter

Source	df	Sum of Squares	Mean Square	R^2	F Ratio
Model	9	201467.35	22385.3	0.89	4.3318
Error	5	25838.25	5167.6		Prob > F
C. Total	14	227305.60			0.0605

Table 4

Lack of Fit Analysis of the Statistical Model Predicting Particle Mean Diameter

Source	df	Sum of Squares	Mean Square	*F* Ratio
Lack of fit	3	17844.250	5948.08	1.4881
Pure error	2	7994.000	3997.00	Prob > F
Total error	5	25838.250		0.4261
				Max RS_q
				0.9648

Table 5

Checkpoint Experiment Comparing Measured to Predicted Response (Size) Using The Statistical Model Shown in Eq. 3

Checkpoint#	X_1	X_2	X_3	Model Mean Diameter (nm)	Measured Mean Diameter (nm)/PDI	Error (%)
1	−0.5	−0.5	0	413.56	393.67/0.345	4.81
2	0.5	0.5	0.5	402.16	397.00/0.445	1.28
3	0.318	0.635	0.199	407.97	377.67/0.357	7.43

Table 6

Particle Mean Diameter, PMD (nm), Polydispersity index (PDI), and Zeta Potential (ζ, mV) of the SLNs using the Optimal Point Obtained from the BBD

Run	PMD/PDI after 1st Layer (PAA)	PMD/PDI after 2nd Layer (PLL)	PMD/PDI after 3rd Layer (Heparin)	ζ after 1st Layer (PAA)	ζ after 2nd Layer (PLL)	ζ after 3rd Layer (Heparin)
1	371/0.334	159/0.441	165/0.473	6.81	55.53	− 55.96
2	361/0.317	346/0.269	165/0.283	9.20	51.16	− 55.06
3	402/0.421	143/0.338	131/0.285	9.00	43.50	− 42.20
Average values ± SEM	378 ± 12.34/0.357 ± 0.032	216 ± 65.16/0.349 ± 0.049	153.66 ± 11.33/0.347 ± 0.063	8.34 ± 0.77	50.06 ± 3.52	− 51.07 ± 4.44